# An Adaptive $T^2$ Chart for Monitoring Dynamic Systems

KAIBO WANG

*Tsinghua University, Beijing 100084, P. R. China*

FUGEE TSUNG

*The Hong Kong University of Science and Technology, Kowloon, Hong Kong*

Although most statistical process control techniques are designed to detect constant process shifts, time-varying shift patterns are more frequently encountered in industrial practice. In this paper, we propose an adaptive $T^2$ scheme for monitoring processes with dynamic shifts. The new scheme preserves the optimality of directionally variant charts by updating a reference mean-shift vector recursively and can be easily adjusted to obtain high sensitivity across desired shift ranges. Simulation studies show that the adaptive $T^2$ chart with EWMA forecasting of mean shifts outperforms most conventional charts in a dynamic environment and is also robust to parameter-estimation uncertainties.

Key Words: Adaptive Chart; Directionally Variant Chart; Exponentially Weighted Moving Average; Hotelling's $T^2$ Statistic; Process Dynamics.

STATISTICAL process control (SPC) techniques have been used widely in a variety of industries. Even though most SPC charts are designed to detect process shifts with constant magnitudes, time-varying shift patterns are frequently encountered in industrial practice. The application of conventional charts to such processes usually results in unsatisfactory performance (Montgomery and Mastrangelo (1991), Tucker et al. (1993), Nembhard and Kao (2003)). Therefore, it is important to investigate the dynamic nature of such processes and introduce new schemes for an efficient detection of the time-varying shift patterns.

The dynamic nature of a process characterizes the way in which the process variables behave, react, and affect each other. Nembhard and Kao (2003) pointed out that a dynamic process, rather than responding to sudden input changes immediately, usually undergoes a substantial transition period before establishing a new process level. For example, in the chemical process studied by Zhang and Pollard (1994) and Runger (2002), abrupt changes in input streams are seen gradually in output streams due to process inertia. The extrusion process described by Nembhard and Kao (2003) exhibits the same feature. Furthermore, the dynamic behavior of continuous processes in modern manufacturing environments has been strengthened by employing short-interval sampling plans (Zhang and Pollard (1994)).

Conventional approaches to monitor a dynamic process usually rely on modifying traditional control charts. Mason and Young (1999) presented a discrete process in which the output variable, $y_t$, followed a first-order autoregressive (AR) model. Instead of monitoring either the process input or process output, a three-dimensional vector, $(x_t, y_{t-1}, y_t)$, which encompasses the one-lagged output, was monitored via a Hotelling $T^2$ chart. Tsung and Apley (2002) investigated the issue of monitoring a feedback-controlled process, which is also a typical dynamic process and strong autocorrelation usually exists between its input and output. The authors

have suggested using a $T^2$ chart,

$$T^2 = \mathbf{v}_t^{\mathrm{T}} \boldsymbol{\Sigma}^{-1} \mathbf{v}_t > h_1, \qquad (1)$$

to monitor vector $\mathbf{v}_t = [y_t, y_{t-1}, \ldots, y_{t-L+1}, x_t, x_{t-1}, \ldots, x_{t-L+1}]^{\mathrm{T}}$, which is a $2L$-dimensional vector of the current and the $(L-1)$-lagged observations of $x_t$ and $y_t$. This is a general $T^2$ chart (denoted as GT2 hereafter) without assuming any prior shift information.

To monitor a vector, it is known that the following projected statistic is expected to be more sensitive to shifts along direction $\mathbf{d}$, given that the future mean-shift direction, $\mathbf{d}$, is exactly known beforehand (Hawkins (1993), Jiang (2004b), Zhou et al. (2005)),

$$T^2 = \mathbf{d}^{\mathrm{T}} \boldsymbol{\Sigma}^{-1} \mathbf{v}_t > h_2. \qquad (2)$$

In contrast to Equation (1), the control chart in Equation (2) is a directionally variant chart because its detection power is dictated not only by the magnitude but also by the direction of a shift. Several extensions to Equation (2) are found in the literature. Jiang (2004a) considered two special forms of Equation (2) in monitoring feedback-controlled processes; Zhou et al. (2005) proposed to use Equations (1) and (2) simultaneously to take care of both general and specific shifts. However, both extensions assumed fixed shift directions; this assumption is obviously violated in a dynamic process.

The purpose of this paper is to provide a novel solution to monitor a general single-input-single-output (SISO) dynamic system without assuming preknown fault directions, but still incorporating dynamic information. The basic idea of the proposed adaptive $T^2$ scheme is. first, to predict the dynamic mean shifts of the process variables and then to adjust the $T^2$ chart adaptively to maximize its power for the predicted shifts. In the rest of this paper, we first analyze the time-varying shift patterns of dynamic processes that follow a general model. Then the adaptive $T^2$ procedure is proposed to handle the challenges of time-varying shifts. The design issues concerning the proposed scheme are also discussed. The performance of the proposed chart is compared with existing charts. The effect of parameter estimation uncertainties is also studied. The last section concludes this paper with some general comments.

## Modeling of Dynamic Systems

As a motivating example, we consider a chemical process that contains a tank with a single input stream and a single output stream, as is shown in
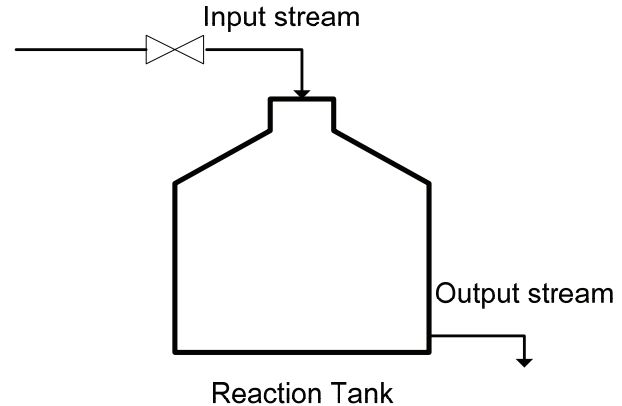


FIGURE 1. A Tank with a Single Input Stream and Single Output Stream.

Figure 1. The input and output streams are two critical factors in this system that have a great impact on the chemical process. Therefore, the statistical monitoring of this system is an important issue in practice (Zhang and Pollard (1994), Montgomery et al. (2000), Runger (2002)). Let $x_t$ be the mass-flow rate into the tank at time $t$ and $y_t$ be the output mass-flow rate at time $t$. It is not difficult to show that the chemical process is characterized by the following generalized model (Zhang and Pollard (1994)):

$$y_t = \delta y_{t-1} + g(1-\delta)x_t + a_t, \qquad (3)$$

where $\delta$ is an inertial parameter that satisfies $0 \leq \delta \leq 1$, which measures the degree of inertia of the process. A large value of $\delta$ corresponds to a slow responding system (Nembhard and Kao (2003)). If $\delta = 0$ holds, no system inertia exists and any changes on the input side, $x_t$, will lead to an immediate full-scale response in $y_t$. The quantity, $g$, is a gain parameter that indicates the impact of changes in $x_t$ on $y_t$. In addition, $a_t \sim N(0, \sigma_a^2)$ is a white-noise series that indicates the disturbance series introduced by the measurement system at time $t$.

The first-order dynamic model in Equation (3) is rather physically representative. Box and Luceno (1997) noted that the dynamic behavior of an industrial system is often approximated quite well by Equation (3). Nembhard and Kao (2003) showed that an extrusion process that produces plastic parts follows Equation (3) in the transient period of a color-change operation. The chemical process demonstrated by Montgomery et al. (2000) is again a special form of Equation (3). The same model is also adopted

by Runger (2002) and Zhang and Pollard (1994) to illustrate a tank process. Tsung et al. (1998) studied a similar model and considered the feedback control issues of this system.

The process input, $x_t$, is assumed to follow an ARMA(1, 1) model, which is expressed as

$$\begin{cases} N_t = \phi N_{t-1} + \varepsilon_t - \theta \varepsilon_{t-1} \\ x_t = \mu_x + N_t, \end{cases} \quad (4)$$

where $\varepsilon_t$ is a white-noise series that satisfies $\varepsilon_t \sim N(0, \sigma_\varepsilon^2)$ and $\mu_x$ is the mean of $x_t$, which is assumed to be zero when the process is in-control. The ARMA(1, 1) model is chosen to cover examples presented in the literature, such as the AR(1) model used by Nembhard and Kao (2003) and Zhang and Pollard (1994), the IMA(1, 1) model adopted by Montgomery et al. (2000), and the ARMA(1, 1) model utilized by Tsung et al. (1998).

Assume that the process is in control, such that $\mu_x = 0$. Substituting Equation (4) for $x_t$ in Equation (3) yields

$$y_t - (\delta + \phi)y_{t-1} + \delta\phi y_{t-2}$$
$$= g(1 - \delta)\varepsilon_t - g(1 - \delta)\theta\varepsilon_{t-1} + a_t - \phi a_{t-1}. \quad (5)$$

The right-hand side of the equation is the sum of two MA(1) series, and $\varepsilon_t$ and $a_t$ are two independent white-noise sequences. As was pointed out by Hamilton (1994), the sum of two MA(1) processes is still an MA(1) process. Therefore, $y_t$ is an ARMA(2, 1) process. As the form of $y_t$ is different from a regular ARMA(2, 1) model, its autocovariance structure is provided in Appendix A.

It is known that a process failure in input and a measurement-system failure in output are two common sources of assignable causes in a dynamic system. We first consider that a sustained shift occurs in the measurement system, which may be caused by incorrectly tuned or broken sensors (Runger (2002)). The failure can be modeled as a mean shift in disturbance process $a_t$, which is expressed by the following model:

$$E(a_t) = \begin{cases} 0 & t < t_0 \\ M(1 - \delta)\sigma_y & t \geq t_0, \end{cases} \quad (6)$$

where $\sigma_y$ is the standard deviation of $y_t$. Under this failure, for $t \geq t_0$, the mean of $y_t$ takes the following form:

$$E[y_t] = M(1 - \delta)\sigma_y \sum_{i=t_0}^{t} \delta^{t-i}, \quad (7)$$

which shows a smoothly increasing trend before reaching a steady state, $M\sigma_y$. As the mean shift in Equation (6) is applied directly to $y_i$, we refer it as a mean shift in $y_t$ in the following discussions.

A simulation example is conducted to investigate the behavior of the process under different mean shifts. We first set $x_0 = y_0 = 0$ and $\varepsilon_0 = 0$. The series, $\varepsilon_t$ and $a_t$, are normally distributed with mean zero and variance one; the sequences of $x_t$ and $y_t$ are then generated according to Equations (4) and (3). Starting from $t_0 = 30$, the mean of $a_t$ shifts to $M = 5.0$. One realization of $y_t$ and $x_t$ under these settings is shown in Figures 2(a) and (c), respectively. It is observed that, although the mean shift of $a_t$ is a constant, the mean of $y_t$ increases gradually before it reaches a stationary level.

We now consider process failures in $x_t$, which may be caused by a sudden raw material change in a chemical process (Nembhard and Kao (2003)). Assume that there is a mean shift of $x_t$ in Equation (4),

$$\mu_x = \begin{cases} 0 & t < t_0 \\ M\sigma_x & t \geq t_0, \end{cases} \quad (8)$$

where $M\sigma_x$ is the new process mean of $x_t$ and $\sigma_x$ is the standard deviation of $x_t$. Consequently, the mean of $y_t$ obeys the following model for $t \geq t_0$:

$$E[y_t] = g(1 - \delta)M\sigma_x \sum_{i=t_0}^{t} \delta^{t-i}, \quad (9)$$

which implies that the mean of $y_t$ increases gradually and approaches its steady level, $Mg\sigma_x$, asymptotically as $t \to \infty$. As the mean shift in Equation (8) is applied directly to $x_t$, we refer to it as a mean shift in $x_t$ in the following discussions.

A realization of $y_t$ under a mean shift in $x_t$ is shown in Figure 2(b). The corresponding input $x_t$ is shown in Figure 2(d). It is observed that the mean shift of $[x_t, y_y]^T$ is $[M\sigma_x, Mg\sigma_x(1 - \delta)]^T$ at step $t_0$ and evolves to $[M\sigma_x, Mg\sigma_x]^T$ as time goes to infinity.

Figure 2 clearly shows the dynamic behavior of the process. Using conventional $T^2$ charts to monitor such a process is less than optimal in the sense that the time-varying shift patterns are not effectively incorporated into the charting scheme. Therefore, this paper proposes an adaptive scheme that uses a recursive forecasting model to predict the time-varying shifts first and then uses a directionally variant chart to monitor the process after that. The details of the scheme are presented in the next section.
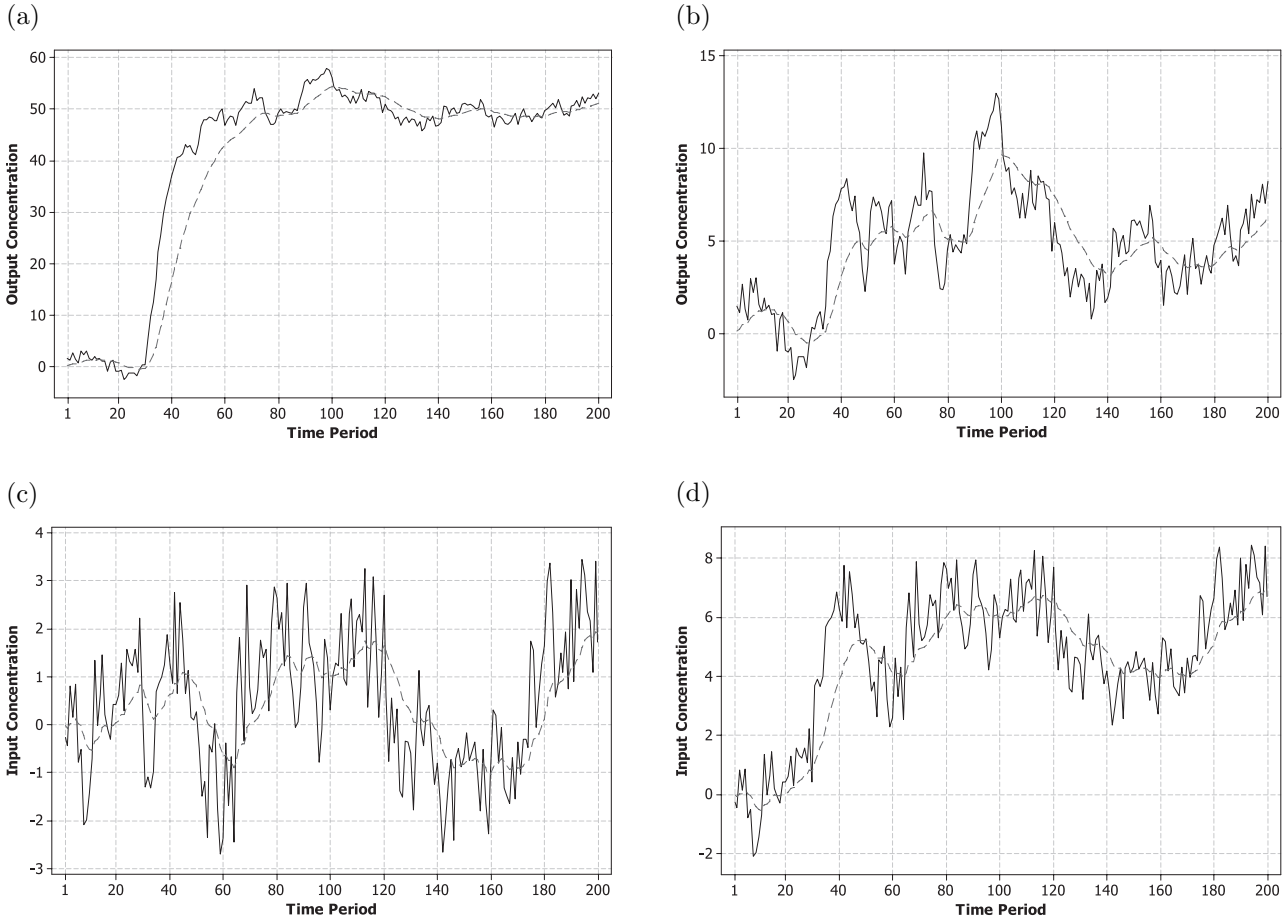
(a)

(b)

(c)

(d)

FIGURE 2. Response of a Dynamic System with $\delta = 0.9$, $g = 1.0$, $\phi = 0.9$, $\theta = 0.5$, $\rho = 0.05$, $M = 5.0$, $\lambda = 0.1$ and $t_0$ = 30. Solid line: output and input streams; dashed line: EWMA prediction. (a) $y_t$ under measurement system shifts, (b) $y_t$ under input level shifts, (c) $x_t$ under measurement system shifts, (d) $x_t$ under input-level shifts.

## An Adaptive $T^2$ Chart

As we can see from Figure 1, when a particular failure occurs, both process inputs and outputs will shift following certain traceable patterns. In light of the directionally variant control chart in Equation (2), we now propose an adaptive $T^2$ procedure to monitor such a dynamic process.

Here we use $\mathbf{v}_t = [y_t, y_{t-1}, \ldots, y_{t-L_1+1}, x_t, x_{t-1}, \ldots, x_{t-L_2+1}]^{\mathrm{T}}$ to denote the vector of $L_1$ successive output observations and $L_2$ input observations. Let $\mathbf{m}_t$ be the predicted mean shift of $\mathbf{v}_t$. At time $t$, we monitor the following statistic and trigger an out-of-control signal when it exceeds the control limit:

$$T^2 = \mathbf{m}_t^{\mathrm{T}} \mathbf{\Sigma}^{-1} \mathbf{v}_t - \frac{1}{2} \mathbf{m}_t^{\mathrm{T}} \mathbf{\Sigma}^{-1} \mathbf{m}_t > h_{\mathrm{AT2}}. \quad (10)$$

This charting statistic can be derived from the log-likelihood ratio with regard to the following hypoth-esis:

$$H_0 : \boldsymbol{\mu}_t = 0 \quad \text{vs.} \quad H_1 : \boldsymbol{\mu}_t = \mathbf{m}_t,$$

where $\boldsymbol{\mu}_t$ is the mean of $\mathbf{v}_t$, $\boldsymbol{\mu}_t = E[\mathbf{v}_t]$. The derivation of Equation (10) is straightforward given the assumption that $\mathbf{V}_t$ follows a multivariate normal distribution with mean $\boldsymbol{\mu}_t$ and covariance matrix $\mathbf{\Sigma}$. The approach of monitoring the likelihood ratio resembles the strategies of Apley and Shi (1999), Jiang (2004b), and Yashchin (1995). More extensive discussions about process monitoring based on the likelihood ratio is given by Basseville and Nikiforov (1993).

The above adaptive $T^2$ chart resembles the directionally variant $T^2$ chart in Equation (2), except that the reference vector, $\mathbf{m}_t$, is subscripted by a time stamp, $t$, and an additional reference term is attached. Because the true mean shift of the process keeps varying over time, the predicted mean shift,
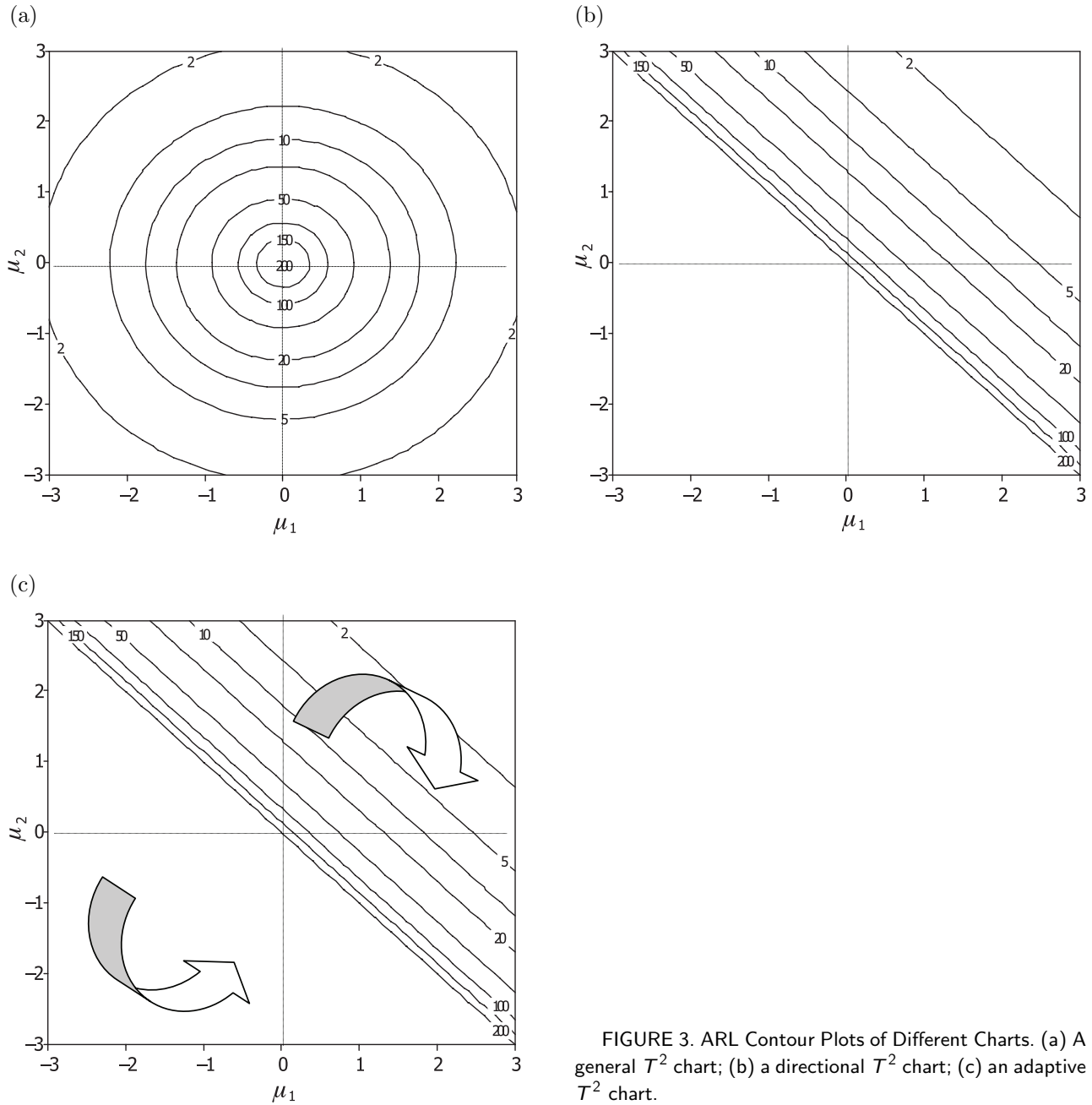
(a)



(b)



(c)



FIGURE 3. ARL Contour Plots of Different Charts. (a) A general $T^2$ chart; (b) a directional $T^2$ chart; (c) an adaptive $T^2$ chart.

$\mathbf{m}_t$, is updated recursively when new observations are collected. This procedure is called adaptive because $\mathbf{m}_t$ is computed recursively and automatically based on the latest observation.

The ARL contour plots of an adaptive $T^2$ chart, a Hotelling $T^2$ chart, and a directionally variant chart, all designed for monitoring a bivariate process with the identity covariance matrix, are presented in Figure 3. The Hotelling's $T^2$ chart exhibits concentric circles, as shown in Figure 3(a); its sensitivity to

shifts is not influenced by shift directions. The directionally variant chart shows parallel lines in Figure (b); the out-of-control ARLs of this chart are determined by both shift magnitudes and shift directions. The minimized out-of-control ARLs are obtained by those shifts along or close to a designated direction. Finally, the adaptive chart performs flexibly, as is shown in Figure 3(c). At any specific step, the adaptive is equivalent to a directionally variant chart. Therefore, the adaptive $T^2$ chart preserves the power

of a directionally variant chart in detecting specific shifts. However, the reference direction of this chart keeps changing over time, which makes it equivalent to rotating the contour plot at each step to emphasize different directions. Therefore, the adaptive $T^2$ chart is expected to be more powerful in detecting dynamic process shifts.

To design and implement the proposed adaptive $T^2$ scheme, several technical issues need to be addressed. First, the referent shift vector, $\mathbf{D}_t$, in Equation (10) needs to be well forecasted. Second, we have to choose an appropriate dimension for $\mathbf{V}_t$. Finally, the control limit needs to be determined based on an acceptable in-control ARL. We will discuss these issues subsequently as follows.

### Forecasting of the Reference Mean Shift

Figure 2 shows the shift patterns of $y_t$ and $x_t$ under various failure conditions. The original mean shifts of the process, however, are buried in the lagged sequences. A successful forecasting scheme should be able to discover the true shifts from collected observations. Although a theoretical description of the dynamic failure patterns can be given by Equations (7) and (9), it is not feasible to predefine the mean shifts by these models. The difficulty lies in the unknown change point from which a failure begins.

Several types of forecasting algorithms have been introduced for autocorrelated processes. When the model of the process is assumed to be known, some researchers suggest using a model-based method to do forecasting (e.g., Montgomery and Mastrangelo (1991), Lin and Adams (1996), Lu and Reynolds (1999), Apley and Shi (1999)). A model-based method usually fits a model to the target process first. Then, the one-step-ahead prediction can be obtained from the model by minimizing the mean square error.

Let $\mathbf{z}_t = [y_t, x_t]^{\mathrm{T}}$ be a vector of the latest observations. Furthermore, let $\mathbf{b}_t = [b_{1,t}, b_{2,t}]^{\mathrm{T}}$ be the one-step-ahead prediction of the process made based on $\mathbf{z}_t$. By referring to Equation (4), $b_{2,t}$ can be expressed as

$$b_{2,t} = E[\tilde{x}_{t+1}] = E[\phi x_t + \varepsilon_{t+1} - \theta\varepsilon_t].$$

Note that $E[\varepsilon_t]$ can be estimated by $E[\varepsilon_t] = x_t - b_{2,t}$ and $E(\varepsilon_{t+1}) = 0$. It follows that

$$b_{2,t} = (\phi - \theta)x_t + \theta b_{2,t-1}. \qquad (11)$$

Based on Equation (3), the one-step-ahead predic-

tion, $b_{1,t}$ can be calculated as

$$b_{1,t} = \delta y_t + g(1 - \delta)b_{2,t}, \qquad (12)$$

or equivalently, as

$$b_{1,t} = \delta y_t + g(1 - \delta)(\phi - \theta)x_t + g(1 - \delta)\theta b_{2,t}. \quad (13)$$

Equations (11) and (13) can be combined in a matrix form as

$$\mathbf{b}_t \begin{pmatrix} \delta & g(1-\delta)(\phi-\theta) \\ 0 & (\phi-\theta) \end{pmatrix} \mathbf{z}_t + \begin{pmatrix} 0 & g(1-\delta)\theta \\ 0 & 0 \end{pmatrix} \mathbf{b}_{t-1}. \tag{14}$$

Once the estimated mean shift of $\mathbf{z}_t$ is known, it can be easily extended to vector $\mathbf{v}_t$. If $L_1$ predicted output shifts and $L_2$ input shifts are kept, the mean shift of $\mathbf{v}_t$ is given by stacking these $L_1 + L_2$ values together,

$$\mathbf{m}_t = [b_{1,t}, b_{1,t-1}, \ldots, b_{1,t-L_1+1}, b_{2,t}, b_{2,t-1}, \ldots,$$
$$b_{2,t-L_2+1}]^{\mathrm{T}}. \tag{15}$$

Based on Equation (15), the adaptive $T^2$ chart can then be implemented.

In contrast, a model-free method does not require explicitly fitting any particular models. One of the most widely used model-free forecasting algorithms is the exponentially weighted moving average (EWMA) procedure. Alwan and Roberts (1989) suggested that the EWMA statistic is a good approximation of time-series models in many cases. A thorough discussion regarding the use of EWMA for forecasting is given by Montgomery and Mastrangelo (1991).

Let $\mathbf{d}_t = [d_{1,t}, d_{2,t}]^{\mathrm{T}}$ be the predicted mean shift of $\mathbf{z}_t$ using EWMA prediction. The recursive updating of $\mathbf{d}_t$ is therefore given by

$$\mathbf{d}_t = \lambda\mathbf{z}_t + (1 - \lambda)\mathbf{d}_{t-1}, \qquad (16)$$

where $\lambda$ is a smoothing parameter that satisfies $0 \leq \lambda \leq 1$. The above procedure is analogous to the multivariate EWMA procedure for monitoring multivariate applications (see Lowry and Montgomery (1995) and references therein). By the same token, the corresponding mean shift of $\mathbf{v}_t$ can be obtained as

$$\mathbf{m}_t = [d_{1,t}, d_{1,t-1}, \ldots, d_{1,t-L_1+1}, d_{2,t}, d_{2,t-1}, \ldots,$$
$$d_{2,t-L_2+1}]^{\mathrm{T}}.$$

The dashed lines in Figure 2 show the estimated mean shift at each step with $\lambda = 0.1$. Although the smoothing parameter usually takes values between zero and one, it is interesting to investigate two extreme cases. Suppose that $\lambda = 1$; the predicted mean shift is given by $\mathbf{d}_t = \mathbf{z}_t$. Therefore,

the predicted sequence is identical to the observation sequence, $\mathbf{m}_t = \mathbf{v}_t$. The adaptive $T^2$ procedure reduces to $T^2 = \mathbf{v}_t^\mathrm{T}\mathbf{\Sigma}^{-1}\mathbf{v}_t/2$, which is equivalent to the conventional $T^2$ chart that ignores the dynamic shift patterns. If instead, $\lambda = 0$, this results in $\mathbf{d}_t = \mathbf{d}_{t-1} = \cdots = \mathbf{d}_0$ and $\mathbf{m}_t = \mathbf{m}_0$. The predicted mean shift actually remains constant at the initial value and is never updated. Under this circumstance, the adaptive procedure is reduced to $T^2 = \mathbf{m}_0^\mathrm{T}\mathbf{\Sigma}^{-1}\mathbf{v}_t - \mathbf{m}_0^\mathrm{T}\mathbf{\Sigma}^{-1}\mathbf{m}_0/2$. As the second term is a constant, the resulting chart is equivalent to the conventional directionally variant $T^2$ chart designed for $\mathbf{m}_0$. In general, the smoothing parameter takes values within $(0,1)$. The procedure is expected both to capture shift trends and to enhance its detection performance.

Even though both the time-series based method and EWMA prediction can be used to estimate process mean shifts, the resulting performance of the adaptive $T^2$ chart may be different. In the next section, the performance of the adaptive $T^2$ chart based on both forecasting algorithms will be studied and the one with better performance will be highlighted.

### The Selection of $L_1$ and $L_2$

In order to select the time-lag parameters, $L_1$ and $L_2$, for the adaptive $T^2$ scheme, we rewrite Equation (4) and express $x_t$ as a function of historical inputs,

$$x_t = -\sum_{k=1}^{\infty}(\theta - \phi)\theta^{k-1}x_{t-k} + e_{xt},$$

which is an AR$(\infty)$ model. The coefficients show the impacts of the historical observations on the current status, which forms a decreasing series as $k$ increases. Apley and Tsung (2002) and Tsung and Apley (2002) suggested selecting the optimal lag length based on the magnitudes of the coefficients. If the magnitude is small enough, the effect of that lagged input on the current observation is negligible. Therefore, the adaptive $T^2$ chart should include historical observations up to the one that has a coefficient larger than a threshold value. By the same token, $y_t$ can be expanded into an AR$(\infty)$ series and the lag length can be determined accordingly. An example of using this technique to choose lag length is presented in the next section.

### A Design Guideline for Practitioners

The control limit of the adaptive $T^2$ chart is determined by process models and other design parameters of the chart, including the in-control ARL. No analytical results are available so far to determine the control limit. Therefore, we provide a computer program that takes necessary parameter values as inputs and automatically searches for a control limit that achieves a desired in-control ARL via numerical simulation. The source code of this computer program and the corresponding executable version is available at http://qlab.ielm.ust.hk/downloads/. The computation of $\mathbf{\Sigma}$, the covariance matrix of $\mathbf{V}_t$, in Equation (10) is needed before setting up the adaptive chart. Because $y_t$ does not follow a regular ARMA(2, 1) model, the computation of the autocovariance of $x_t$, $y_t$, as well as the covariance between them, are sketched in Appendix A to Appendix C. The covariance matrix, $\mathbf{\Sigma}$, can also be computed and displayed by the computer program.

The following procedures are suggested to be followed by practitioners to design and implement the adaptive $T^2$ chart:

Step 1: Collect samples from the process with a certain sample size (which will be discussed in the next section).

Step 2: Estimate process autocorrelations and choose appropriate lag lengths for the control chart.

Step 3: Based on the magnitude of interested shifts, choose a smoothing parameter for EWMA if EWMA prediction is adopted; then based on an acceptable in-control ARL, determine a control limit. The calculation of the control limit can be done using the numerical method provided by our computer program (as mentioned above).

Step 4: Set up the chart and apply it on-line.

## Performance Analysis

To study the performance of the proposed procedure, multivariate EWMA (MEWMA), multivariate CUSUM (MCUSUM), and the general $T^2$ chart (GT2) in Equation (1) are compared with the proposed adaptive $T^2$ chart (AT2). Similar to the AT2 chart, the GT2 chart may use different numbers of lagged observations, as discussed by Tsung and Apley (2002). The MEWMA has been proven in the literature (Lowry et al. (1992)) to be sensitive to small process shifts. The chart calculates

$$\mathbf{w}_t = \lambda\mathbf{z}_t + (1 - \lambda)\mathbf{w}_{t-1}, \qquad (17)$$

with $\mathbf{w}_0 = 0$ and signals if

$$T_{\mathrm{ME}}^2 = \mathbf{w}_t^\mathrm{T}\mathbf{\Sigma}^{-1}\mathbf{W}_t > h_{\mathrm{ME}}, \qquad (18)$$

where $h_{ME}$ is chosen to achieve a specified in-control ARL.

There are several schemes available for the MCUSUM procedure. Among others, the one proposed by Woodall and Ncube (1985) uses multiple univariate CUSUM charts simultaneously to monitor process variables. In the following study, we apply this MCUSUM chart to the target process. Both input and output streams are monitored by a double-sided univariate CUSUM chart. The tabular form of the charts is given by

$$
\begin{cases}
C^+_{y,t} = \max(0, C^+_{y,t-1} + y_t - k) \\
C^-_{y,t} = \max(0, C^-_{y,t-1} - y_t - k) \\
C^+_{x,t} = \max(0, C^+_{x,t-1} + x_t - k) \\
C^-_{x,t} = \max(0, C^-_{x,t-1} - x_t - k),
\end{cases}
$$

and the MCUSUM chart triggers an alarm if the following condition is satisfied:

$$
\max(C^+_{y,t}, C^-_{y,t}) > h_y \quad \text{or} \quad \max(C^+_{x,t}, C^-_{x,t}) > h_x, \tag{19}
$$

where $h_y$ and $h_x$ are the control limits for the two double-sided univariate CUSUM charts. Let the in-control ARL of each univariate CUSUM chart be $\mathrm{ARL}^y_0$ and $\mathrm{ARL}^x_0$, respectively. The control limits, $h_y$ and $h_x$, should guarantee $\mathrm{ARL}^y_0 = \mathrm{ARL}^x_0$. In addition, the overall in-control ARL obtained from Equation (19) should satisfy a specified value.

Based on the forecasting algorithms presented in Equations (14) and (16), two different AT2 charts are presented. We denote the AT2 chart based on one-step-ahead forecasting as the AT2-OSA chart and the AT2 chart based on EWMA forecasting as the AT2-E chart. The true values of the process parameters are assumed to be known in the following study. The influence of parameter estimation uncertainties on the adaptive $T^2$ chart will be studied in the sensitivity-analysis section.

Steady-state ARLs are selected as indices for comparison. The steady-state ARL is computed assuming the process has reached its steady state, which is a way to remove the initial-state bias caused by assuming zero states for all process variables when the process starts up (Apley and Tsung (2002)). In the following study, $t_0 = 100$ is used in Equations (6) and (8) because it is learned from Equation (4) when $\nu_x = 0$ that

$$
x_t = \phi^t x_0 + \varepsilon_t + (1-\theta) \sum_{k=1}^{t-1} \varepsilon_{t-k} - \theta \varepsilon_0. \tag{20}
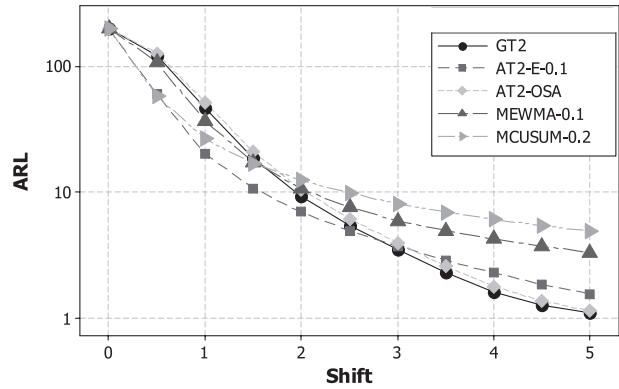$$

This choice guarantees that the inertial state of the



FIGURE 4. ARL Performance Comparison. (a) A general $T^2$ chart, (b) a directional $T^2$ chart, (c) an adaptive $T^2$ chart.

process, $x_0$, has a negligible impact on the resulting ARLs.

Monte Carlo simulations are carried out to calculate the ARLs; each ARL value is obtained using at least 10,000 replicates. For a fair comparison, the control limit of each chart is tuned to achieve an in-control ARL of 200.0. The simulated process has the following settings: $\delta = 0.9$, $\phi = 0.5$, $\theta = 0.0$, $g = 1$, $\sigma^2_a = \sigma^2_\varepsilon = 1.0$. Based on a study on the autocorrelation function of $x_t$ and $y_t$, $x_t$ is found to be correlated with itself up to 3 lags and $y_t$ up to 15 lags. Therefore, we choose the lag combination of $(L_1, L_2) = (16, 4)$ as the optimal one. However, other combinations are also considered for comparison.

Figure 4 graphically compares the AT2 scheme with GT2, MEWMA, and MCUSUM charts. In specific, the lag combination $(L_1, L_2) = (16, 4)$ is chosen for the AT2 and GT2 charts. AT2 uses EWMA forecasting with $\lambda = 0.1$, MEWMA uses $\lambda = 0.1$, and MCUSUM uses $k = 0.2$ as a reference value. It is clearly seen from the graph that MCUSUM and AT2-E charts outperform other schemes for small mean shifts, while MCUSUM and MEWMA charts have relatively poor large-shift performance. GT2 performs the best in detecting large shifts, which is not unexpected. However, we should favor the AT2-E chart if an overall performance is of concern because it demonstrates a satisfactory performance for both small and large shifts.

More detailed results are shown in Tables 1 and 2. Table 1 shows the estimated ARLs of the two adaptive $T^2$ charts. The AT2 chart based on EWMA

TABLE 1. Estimated ARLs of the AT2-E and AT2-OSA Charts. $\delta = 0.9$, $\phi = 0.5$, $\theta = 0.0$, $g = 1$, $\sigma_a^2 = \sigma_\varepsilon^2 = 1.0$

| | AT2-E | | | | | | AT2-OSA | | |
|---|---|---|---|---|---|---|---|---|---|
| | $\lambda = 0.1$ | | | $\lambda = 0.5$ | | | | | |
| $(L_1, L_2)$ | (2,2) | (10,10) | (16,4) | (2,2) | (10,10) | (16,4) | (2,2) | (10,10) | (16,4) |
| $h_{\text{AT2}}$ | 2.792 | 4.199 | 4.236 | 5.607 | 12.481 | 12.384 | 6.176 | 15.482 | 14.340 |
| ARLs with shifts in $x_t$ (Equation (8)) | | | | | | | | | |
| $M = 0.0$ | 200.24 (205.3) | 200.05 (206.0) | 200.22 (205.9) | 200.93 (206.8) | 200.17 (207.6) | 199.67 (205.0) | 200.87 (206.9) | 200.34 (205.9) | 199.32 (204.5) |
| 0.5 | 83.41 (79.7) | 65.06 (61.2) | 60.15 (55.8) | 113.40 (114.0) | 114.79 (117.0) | 100.18 (100.5) | 146.75 (147.9) | 145.98 (146.9) | 127.39 (128.5) |
| 1.0 | 27.93 (22.8) | 21.53 (16.8) | 20.26 (14.9) | 42.95 (42.6) | 41.13 (39.8) | 33.41 (31.3) | 70.35 (69.9) | 69.32 (69.8) | 51.77 (49.5) |
| 1.5 | 13.30 (9.5) | 10.92 (7.1) | 10.73 (6.5) | 17.77 (16.8) | 16.30 (14.5) | 14.06 (11.3) | 30.60 (30.5) | 30.32 (29.4) | 20.98 (18.1) |
| 2.0 | 7.89 (5.2) | 7.03 (4.1) | 6.97 (3.9) | 8.15 (7.9) | 8.11 (6.8) | 7.40 (5.4) | 14.00 (13.7) | 13.85 (12.7) | 10.55 (8.0) |
| 2.5 | 5.28 (3.3) | 4.95 (2.7) | 4.95 (2.7) | 4.37 (4.2) | 4.78 (3.7) | 4.56 (3.3) | 6.63 (6.9) | 7.39 (6.3) | 6.17 (4.4) |
| 3.0 | 3.84 (2.3) | 3.73 (2.0) | 3.75 (2.0) | 2.50 (2.3) | 2.99 (2.3) | 2.95 (2.2) | 3.62 (3.9) | 4.42 (3.5) | 3.96 (3.0) |
| 3.5 | 2.94 (1.7) | 2.87 (1.6) | 2.88 (1.5) | 1.66 (1.4) | 2.06 (1.5) | 1.99 (1.4) | 2.03 (2.0) | 2.89 (2.2) | 2.59 (2.0) |
| 4.0 | 2.31 (1.4) | 2.29 (1.2) | 2.30 (1.2) | 1.24 (0.7) | 1.52 (1.0) | 1.49 (0.9) | 1.37 (1.0) | 1.96 (1.5) | 1.79 (1.3) |
| 4.5 | 1.87 (1.1) | 1.82 (0.9) | 1.85 (1.0) | 1.07 (0.4) | 1.23 (0.6) | 1.22 (0.6) | 1.12 (0.5) | 1.46 (0.9) | 1.37 (0.8) |
| $M = 5.0$ | 1.54 (0.9) | 1.52 (0.7) | 1.55 (0.8) | 1.02 (0.2) | 1.09 (0.3) | 1.08 (0.3) | 1.03 (0.2) | 1.20 (0.6) | 1.14 (0.5) |
| ARLs with shifts in $y_t$ (Equation (6)) | | | | | | | | | |
| $M = 0.0$ | 200.24 (205.3) | 200.05 (206.0) | 200.22 (205.9) | 200.93 (206.8) | 200.17 (207.6) | 199.67 (205.0) | 200.87 (206.9) | 200.34 (205.9) | 199.32 (204.5) |
| 0.5 | 132.79 (131.7) | 139.17 (137.6) | 142.92 (141.6) | 155.66 (154.7) | 167.28 (170.1) | 170.21 (175.2) | 159.58 (160.9) | 173.39 (176.3) | 174.66 (174.8) |
| 1.0 | 68.11 (62.0) | 73.66 (67.4) | 76.11 (70.4) | 91.97 (87.1) | 111.03 (106.2) | 116.66 (114.3) | 96.50 (91.1) | 123.83 (121.1) | 125.46 (124.0) |
| 1.5 | 39.39 (31.3) | 42.49 (34.2) | 43.87 (36.0) | 54.00 (47.5) | 69.40 (63.4) | 75.38 (70.1) | 57.57 (50.6) | 80.24 (74.6) | 83.15 (77.7) |
| 2.0 | 26.13 (18.6) | 27.97 (20.0) | 28.70 (20.8) | 34.28 (26.5) | 44.70 (37.2) | 48.34 (41.5) | 36.66 (29.3) | 52.95 (45.4) | 54.70 (47.2) |
| 2.5 | 19.20 (12.0) | 20.26 (13.1) | 20.67 (13.6) | 24.17 (17.4) | 31.01 (23.5) | 32.88 (25.9) | 25.54 (18.4) | 36.80 (28.7) | 37.41 (30.0) |
| 3.0 | 15.20 (8.8) | 15.82 (9.4) | 16.17 (9.6) | 17.97 (11.7) | 22.88 (16.1) | 23.98 (17.6) | 18.96 (12.6) | 26.80 (19.1) | 26.99 (20.0) |
| 3.5 | 12.55 (6.6) | 13.06 (7.3) | 13.46 (7.3) | 14.33 (8.6) | 17.69 (11.7) | 18.58 (12.7) | 15.14 (9.3) | 20.56 (13.7) | 20.65 (14.0) |
| 4.0 | 10.74 (5.3) | 10.88 (5.8) | 11.33 (5.8) | 11.70 (6.6) | 14.07 (8.9) | 14.87 (9.3) | 12.30 (7.1) | 16.39 (10.6) | 16.45 (10.5) |
| 4.5 | 9.44 (4.4) | 9.41 (4.9) | 9.81 (4.8) | 9.93 (5.3) | 11.66 (7.2) | 12.32 (7.4) | 10.28 (5.6) | 13.36 (8.2) | 13.65 (8.3) |
| $M = 5.0$ | 8.52 (3.8) | 8.25 (4.1) | 8.79 (4.2) | 8.57 (4.5) | 9.81 (5.9) | 10.33 (6.1) | 8.88 (4.7) | 11.25 (6.8) | 11.44 (6.7) |

forecasting (AT2-E chart) uses either $\lambda = 0.1$ or $\lambda = 0.5$. The corresponding control limits, $h_{\text{AT2}}$, are also shown. Two types of process failures are introduced into the process. The upper part of Table 1 contains the results when the shift that follows Equation (8) occurs in $x_t$. The lower part gives the ARLs of the charts when the process is subject to shifts that follows Equation (6).

We first investigate the upper part of Table 1, which indicates the performance of the charts with $x_t$ shifts. Compared with the AT2-E chart with $\lambda = 0.1$, no matter which lag combination is utilized, the AT2-OSA chart is always inferior to the AT2-E chart for small and moderate shifts. Only when the shift increases does the performance of the AT2-OSA chart become better. This phenomenon suggests that, analogous to other EWMA-based control charts, the EWMA forecasting in AT2-E has an ef-

fect of accumulating small shifts, which in turn contributes to the fast detection of them. A careful investigation at Equation (11), which can be rewritten as $b_{2,t} = (1 - \theta)x_t + \theta b_{2,t-1} + (\phi - 1)x_t$, reveals that the one-step-ahead prediction of process input is the summarization of an EWMA smoothed term plus a scaled $x_t$. However, a further look at Equation (12), $b_{1,t} = \delta y_t + g(1 - \delta)b_{2,t}$, clearly shows that the one-step-ahead prediction of process output is made by combining $y_t$ and $b_{2,t}$. Historical process outputs, $y_{t-k}$, $k \geq 1$, are not included in this equation (even though historical $x$'s are preserved by $b_{2,t-1}$). Therefore, $y_t$ is updated based on the most recent output (and historical inputs) only. As a result, the AT2-OSA chart does not fully take advantage of historical information and loses sensitivity when detecting small shifts. In addition, the one-step-ahead method in Equation (14), which is derived by assuming $\mu_x = 0$ in Equation (4), does not take

TABLE 2. Estimated ARLs of the AT2-E and AT2-OSA Charts. $\delta = 0.9$, $\phi = 0.5$, $\theta = 0.0$, $g = 1$, $\sigma_a^2 = \sigma_\varepsilon^2 = 1.0$

| | GT2 | | | MEWMA | | MCUSUM | | |
|---|---|---|---|---|---|---|---|---|
| | $(L_1, L_2)$ | | | $\lambda$ | | $k$ | | |
| | (2,2) | (10,10) | (16,4) | 0.1 | 0.5 | 0.2 | 0.5 | 1.0 |
| | $h_{\mathrm{GT2}}$ | | | $h_{\mathrm{ME}}$ | | $(h_{s1}, h_{s2})$ | | |
| | 14.122 | 35.558 | 35.191 | 2.151 | 6.233 | (9.454, 24.352) | (4.949, 13.677) | (2.602, 6.909) |
| ARLs with shifts in $x_t$ (Equation (8)) | | | | | | | | |
| $M = 0.00$ | 200.58 (204.8) | 200.41 (203.1) | 200.02 (203.6) | 199.59 (211.8) | 199.58 (205.64) | 199.23 (168.5) | 200.13 (190.0) | 199.61 (197.4) |
| 0.50 | 132.57 (132.7) | 136.84 (138.2) | 122.08 (122.5) | 108.10 (108.2) | 111.48 (113.11) | 57.76 (31.9) | 59.02 (46.7) | 76.62 (71.9) |
| 1.00 | 57.19 (57.4) | 58.78 (58.2) | 46.83 (45.2) | 36.70 (30.9) | 40.14 (38.66) | 26.68 (10.2) | 21.25 (11.7) | 23.09 (18.4) |
| 1.50 | 23.53 (23.0) | 24.09 (23.2) | 18.74 (16.4) | 17.38 (11.6) | 16.60 (15.10) | 16.89 (5.1) | 12.41 (5.4) | 10.73 (6.9) |
| 2.00 | 10.54 (10.7) | 10.85 (9.9) | 9.38 (7.3) | 10.68 (5.9) | 7.92 (6.82) | 12.46 (3.2) | 8.55 (3.0) | 6.52 (3.4) |
| 2.50 | 4.99 (5.4) | 5.93 (4.9) | 5.47 (4.1) | 7.60 (3.8) | 4.78 (3.73) | 9.85 (2.2) | 6.53 (1.9) | 4.64 (2.0) |
| 3.00 | 2.65 (2.8) | 3.57 (2.9) | 3.49 (2.7) | 5.92 (2.6) | 3.13 (2.06) | 8.11 (1.6) | 5.31 (1.4) | 3.58 (1.3) |
| 3.50 | 1.64 (1.5) | 2.34 (1.8) | 2.29 (1.8) | 4.96 (2.0) | 2.38 (1.34) | 6.96 (1.2) | 4.51 (1.0) | 2.94 (0.9) |
| 4.00 | 1.22 (0.8) | 1.65 (1.2) | 1.62 (1.2) | 4.24 (1.7) | 1.92 (0.93) | 6.11 (1.0) | 3.92 (0.8) | 2.51 (0.7) |
| 4.50 | 1.06 (0.3) | 1.29 (0.7) | 1.26 (0.7) | 3.72 (1.4) | 1.64 (0.69) | 5.43 (0.8) | 3.49 (0.7) | 2.23 (0.5) |
| $M = 5.00$ | 1.01 (0.2) | 1.10 (0.4) | 1.10 (0.4) | 3.33 (1.2) | 1.44 (0.57) | 4.93 (0.7) | 3.16 (0.5) | 2.07 (0.4) |
| ARLs with shifts in $y_t$ (Equation (6)) | | | | | | | | |
| $M = 0.0$ | 200.58 (204.8) | 200.41 (203.1) | 200.02 (203.6) | 199.59 (211.8) | 199.58 (205.6) | 199.23 (168.5) | 200.13 (190.0) | 199.61 (197.4) |
| 0.5 | 162.83 (163.7) | 177.32 (180.0) | 181.45 (184.4) | 120.98 (121.8) | 140.37 (137.0) | 145.12 (116.9) | 168.52 (156.9) | 182.65 (179.9) |
| 1.0 | 103.54 (98.9) | 130.52 (126.7) | 137.50 (136.9) | 59.47 (52.7) | 73.90 (69.7) | 78.90 (56.3) | 108.28 (99.0) | 143.63 (138.3) |
| 1.5 | 63.21 (56.7) | 87.25 (81.1) | 97.05 (93.8) | 34.73 (26.8) | 42.16 (35.3) | 47.52 (29.8) | 63.59 (56.2) | 102.28 (97.9) |
| 2.0 | 40.47 (32.6) | 58.16 (50.7) | 65.27 (58.6) | 24.20 (16.0) | 27.30 (20.6) | 32.11 (17.0) | 39.60 (32.3) | 69.55 (65.8) |
| 2.5 | 28.04 (20.4) | 40.38 (32.0) | 44.48 (37.2) | 18.60 (10.9) | 19.66 (13.4) | 24.18 (11.6) | 26.22 (19.8) | 46.85 (44.2) |
| 3.0 | 20.81 (13.9) | 29.44 (21.3) | 31.97 (24.3) | 15.21 (8.0) | 15.19 (9.3) | 19.20 (8.1) | 18.73 (12.6) | 32.01 (28.9) |
| 3.5 | 16.40 (10.0) | 22.65 (15.2) | 24.26 (17.2) | 13.02 (6.2) | 12.21 (6.9) | 15.95 (6.2) | 14.40 (8.9) | 22.28 (19.4) |
| 4.0 | 13.24 (7.5) | 17.97 (11.4) | 19.13 (12.7) | 11.55 (5.2) | 10.36 (5.4) | 13.62 (4.8) | 11.46 (6.5) | 16.14 (13.7) |
| 4.5 | 11.24 (6.1) | 14.76 (9.1) | 15.58 (9.6) | 10.50 (4.6) | 8.95 (4.3) | 11.93 (4.0) | 9.43 (4.8) | 12.15 (9.8) |
| $M = 5.0$ | 9.61 (5.0) | 12.25 (7.3) | 13.19 (7.8) | 9.71 (4.0) | 7.92 (3.6) | 10.54 (3.3) | 8.12 (3.8) | 9.60 (7.2) |

process mean shifts into account. Therefore, when a shift exists in the process, its forecasting performance is rather poor.

It should be noted that the ARL performance of the AT2-E chart is also influenced by $\lambda$. As is seen from the upper part of Table 1, the large-shift performance of the AT2-E is improved when $\lambda = 0.5$ is used. Although in the mean time, the ARLs of the AT2-E chart corresponding to small shifts deteriorate, a careful examination reveals that the AT2-E with $\lambda = 0.5$ is favored over the AT2-OSA chart, as the former chart outperforms the latter one in a large shift range. This finding suggests that the AT2-E chart is rather flexible in design. The smoothing parameter, $\lambda$, can be adjusted according to different shift ranges of interest. A small $\lambda$ helps boost the performance of the chart for small shifts, while a large $\lambda$ improves the large shift performance.

Finally, the AT2-E chart with lag combination $(16, 4)$ gives reasonably good overall performance, which implies that the strategy of choosing lag combinations based on the process autocorrelation structure gives satisfactory results.

The lower part of Table 1 shows the performance of the charts when $y_t$ shifts. We know from Equation (7) that a mean shift of size $M\sigma_y(1-\delta)$ in the disturbance sequence will cause the mean of $y_t$ to increase to $M\sigma_y$. In the table, the value of $M$ is shown to indicate the shift magnitude. In general, the relationships among the charts when $y_t$ shifts are similar to

those when $x_t$ shifts. The AT2-E chart outperforms the AT2-OSA chart in most cases.

Table 2 shows the ARL performance of the GT2, MEWMA, and MCUSUM charts. As AT2-E and AT2-OSA have been investigated, we will first investigate the performance of the charts in Table 2 and then compare them with only the AT2-E chart in Table 1.

We can see from Table 2 that the GT2 chart is advantageous compared with other charts in detecting large shifts in most cases. This is a known property of Shewhart-type control charts. However, its performance with small shifts is nearly the worst among all the charts. Compared with the GT2 chart, both the MEWMA and CUSUM charts have improved small-shift performance. When comparing across Table 2 and Table 1, it is clearly seen that the AT2-E chart is always advantageous compared with the GT2 chart for detecting small and moderate shifts. Although the large-shift performance of the AT2-E chart is not as good as that of the GT2 chart, increasing $\lambda$ will help to reduce the gap. The findings are in agreement with the previous analysis. As the GT2 chart is a special AT2-E chart with $\lambda = 1.0$, their performances will be close if $\lambda$ is close to one.

A comparison between AT2-E and MEWMA shows that, although the MEWMA chart has improved small-shift performance, it is still inferior to the AT2-E chart for all shifts in $x_t$ and for large shifts in $y_t$. To compare the AT2-E charts with the MCUSUM charts, we focus on the shifts in $x_t$ first. It is seen that the AT2-E chart with $\lambda = 0.1$ and lag combination $(16, 4)$ outperforms the MCUSUM chart with $k = 0.2$ for nearly all shifts except those with magnitudes around 0.5. The AT2-E chart also outperforms the CUSUM chart with $k = 1.0$ in detecting small and large shifts but not moderate shifts with magnitudes between 2.0 and 3.5. These findings are explained by the fact that a CUSUM chart is quick in detecting shifts within a certain range, which is determined by the reference value it uses. The MCUSUM chart with $k = 0.2$ is sensitive to small process shifts, while the MCUSUM chart with $k = 1.0$ gives the fastest detection of shifts with a moderate level. When shifts in $y_t$ occur, the performance of the AT2-E chart with $\lambda = 0.1$ is even more profound. It performs better than the MCUSUM charts with $k = 0.2$ and $k = 1.0$ for all shifts and is only slightly worse than MCUSUM with $k = 0.5$ for shifts around 5.0. Generally speaking, as the shift pattern of the process is time varying, the MCUSUM

chart that uses a constant reference value cannot achieve the best performance over all shifts. However, the AT2 chart adjusts itself automatically according to the underlying shifts and is more favored if the overall performance is of interest.

## The Effect of Estimating Process Parameters

In the previous section, we conducted our analyses based on the assumption that process parameters are precisely known for control-chart design. However, real situations are always encountered when the true values of parameters are not known exactly. A theoretical framework is usually implemented by replacing true values with estimated ones. As a result, the performance of a control chart may not be as good as expected (Lu and Reynolds (1999), Jones et al. (2004), Shu et al. (2004)). One desirable property of control charts is robustness to parameter-estimation uncertainties. In this section, we focus on the AT2-E and AT2-OSA charts and investigate their ARL performance under parameter-estimation uncertainties.

In the following study, the true values of the parameters are taken the same as in the previous studies. However, when setting up the control chart, estimated parameters are used. The following procedures illustrate how the simulations are conducted:

1. A sample of size $m$ is generated, which contains $[x_t, y_t]$, $1 \le t \le m$.

2. Based on Equations (3) and (4), all process parameters are estimated from the above samples.

3. The AT2-E and AT2-OSA charts are designed based on estimated parameters to achieve an in-control ARL of 200.0.

4. Both charts are set up to monitor the process, and the resulting in-control ARLs and out-of-control ARLs are estimated.

5. Go back to the first step until 100 replicates are finished.

Simulation results are shown in Figure 5. For each shift magnitude, the box plot of 100 replicates is drawn. The middle solid box shows the first and the third quartiles of the data. The median values of the ARLs of all shifts are connected by a solid line. To show the influence of the sample size, $m$ takes the values of 100, 500, and 1000.

Figure 5 indicates that, when the chart is designed based on estimated parameters, a very large or small in-control ARL may be seen. For example, in Figure 5(a), the parameters are estimated with 100 samples.
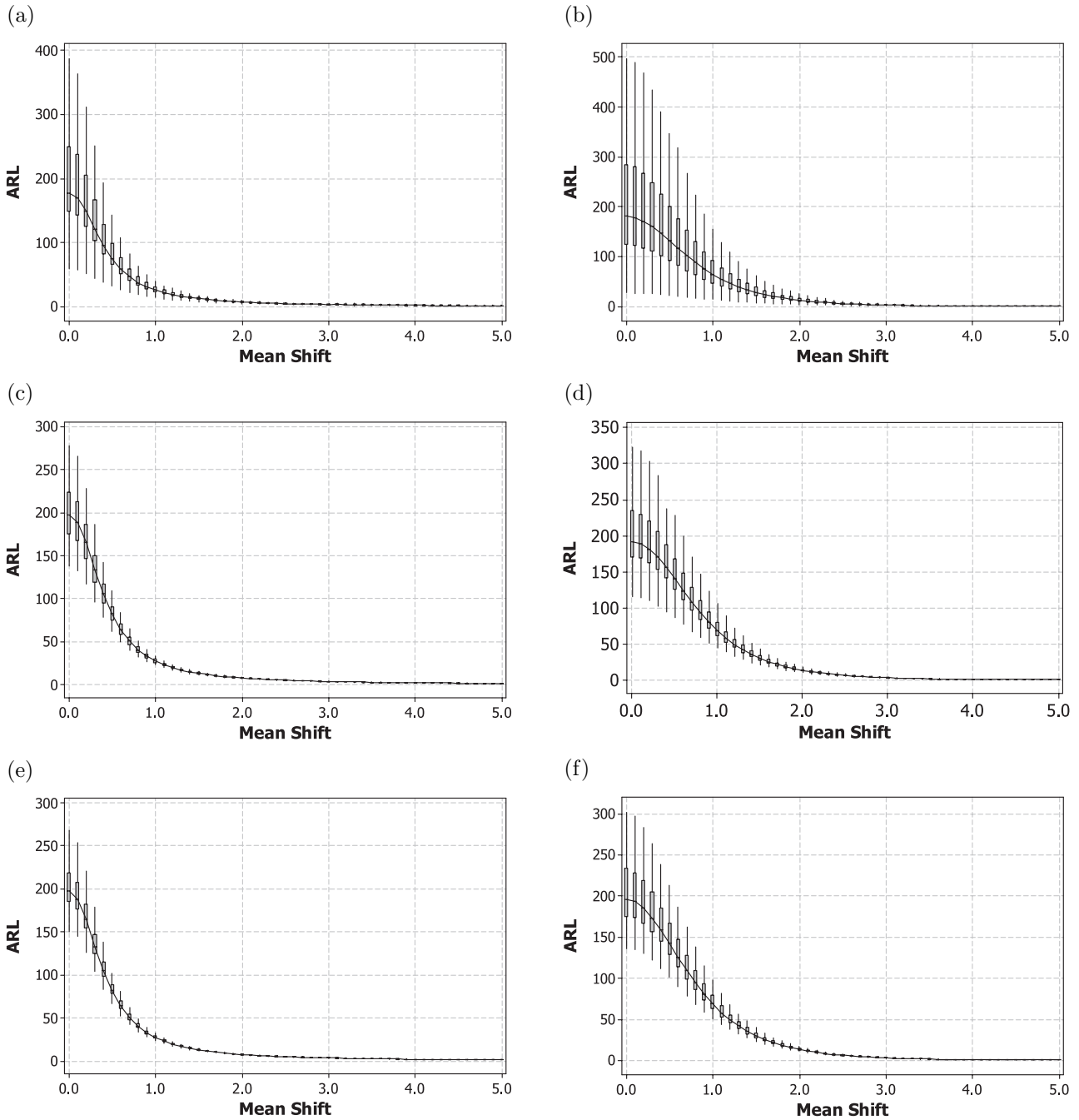
FIGURE 5. Estimated ARLs of AT2-E and AT2-OSA Charts Under Parameter Estimation Uncertainties. (a) AT2-E, $m =$ 100; (b): AT2-OSA, $m = 100$; (c): AT2-E, $m = 500$; (d): AT2-OSA, $m = 500$; (e): AT2-E, $m = 1000$; (f): AT2-OSA, $m =$ 1000.

It turns out that around one quarter of the AT2-E charts have in-control ARLs larger than 249 and one quarter less than 150. Accordingly, the out-of-control ARLs spread out widely around the mean values. When the sample size increases, the spreads of both in-control and out-of-control ARLs narrow. A significant improvement is seen when 1000 samples are used in parameter estimation. Similar to the
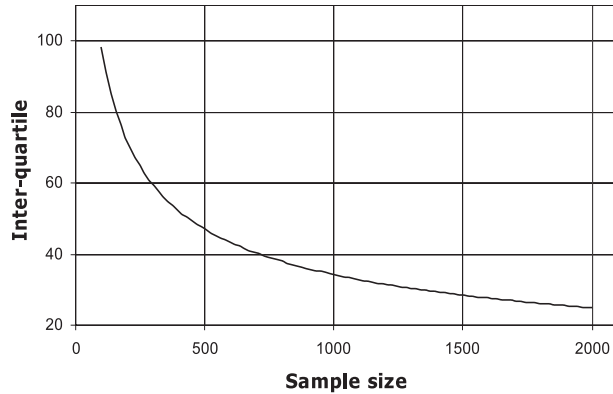
FIGURE 6. The Interquartile Plot of the In-Control ARLs of the AT2-E Chart.

conclusions drawn in Lu and Reynolds (1999), the typical level of 100 samples in parameter estimation is inadequate in the inertial process.

The uncertainties in the AT2-OSA charts are also shown in Figure 5. Although the variance of the ARLs decreases when $m$ increases, it is clearly seen that the AT2-OSA chart has much larger interquartile values than the corresponding AT2-E charts that use an equal sample size. Therefore, parameter estimation uncertainties have more profound impacts on the model-based AT2-OSA chart than on the AT2-E chart.

As studies on residual-based monitoring schemes are seen in the literature, we may also compare the AT2 chart with those methods. However, the major issue with residual-based methods is the existence of parameter-estimation uncertainties. When process parameters are not estimated accurately, the resulting residual sequence could be a very complex process; in this situation, the real monitoring performance might be hard to predict. However, the AT2-E chart avoids such risks by using the EWMA forecasting algorithm, which is robust to such uncertainties.

Figure 6 shows the interquartile, which is the distance between the first and the third quartiles, of the in-control ARL of the AT2-E charts. It is seen that the interquartile slopes down sharply when the sample size is less than 500, then slopes down slowly when the sample size is larger than 500. A choice of 500 or more samples will guarantee that the true in-control ARL of the chart is within $\pm 12\%$ of the expected one. Therefore, a sample size of 500 or more is recommended for practitioners to gain a reliable estimate of the in-control ARL.

Extensive simulations with processes that have other parameter settings have been conducted as well. We observe very similar trends in these results and conclude that the superiority and robustness of the AT2 chart hold in general.

## Conclusion

With the presence of time-varying shifts in a process, it is important to incorporate these shift patterns into control-chart design. In this paper, we have proposed an adaptive $T^2$ chart, which uses forecasting algorithms to predict process mean shifts first and then adjusts itself to enhance its power in detecting the predicted shifts.

Both model-based and model-free forecasting algorithms have been investigated in this study. The AT2-E chart has been proven to be superior to the AT2-OSA chart in most cases. In addition, the AT2-E chart is flexible in design. The smoothing parameter can be easily tuned for fast detection of either small, moderate, or large shifts. In particular, a small $\lambda$ gives better detection of small shifts, while a large $\lambda$ enhances the large-shift detection performance. More important, AT2-E is more robust to parameter-estimation uncertainties than AT2-OSA. Therefore, the AT2-E chart is recommended for practitioners in a dynamic environment.

When process parameters are estimated from historical samples, the choice of the sample size for parameter estimation is important in chart design. We have conducted a sensitivity analysis and revealed that the conventional choice of 100 samples seems inadequate for the dynamic process studied in this paper. Instead, a choice of 500 samples or more is recommended for a reliable chart design.

The diagnostic properties of the adaptive $T^2$ chart were not discussed in this paper. Analogous to other multivariate control charts, the methods proposed by Hawkins (1993) and Mason et al. (1995) are good candidates for this purpose.

Although the adaptive $T^2$ chart was studied on the basis of SISO processes in this paper, it can be extended to feedback-controlled processes and other general multivariate applications. Wang and Tsung (2007) applied the adaptive $T^2$ chart to feedback-controlled processes and proposed using an oscillated-EWMA method for shift forecasting. Extensions to other real scenarios and design of case-dependent forecasting algorithms are interesting topics that deserve future research attention.

## Acknowledgments

## Appendix A
## The Autocovariance Structure of the Output Process

For convenience, Equation (5) can be rewritten as

$$y_t(1-\delta B)(1-\phi B) = g(1-\delta)(1-\theta B)\varepsilon_t + (1-\phi B)a_t,$$

where $B$ is the backshift operator such that $By_t = y_{t-1}$. Let $\phi_1 = \delta + \phi$, $\phi_2 = -\delta\phi$, $\kappa = g(1-\delta)$. The above ARMA(2, 1) model can be expressed as

$$y_t = \phi_1 y_{t-1} + \phi_2 y_{t-2} + \kappa\varepsilon_t - \kappa\theta\varepsilon_{t-1} + a_t - \phi a_{t-1}. \tag{A1}$$

Multiply both sides of Equation (A1) by $y_t$, $y_{t-1}$, $y_{t-2}$, $\varepsilon_t$, $\varepsilon_{t-1}$, $a_t$, and $a_{t-1}$. Determine the expectation and note that $e[y_k\varepsilon_t] = E[y_k a_t] = 0$ for $k < t$. The following equations are obtained:

$$\begin{cases} r_{y0} = \phi_1 r_1 + \phi_2 r_2 + \kappa E[y_t\varepsilon_t] - \kappa\theta E[y_t\varepsilon_{t-1} \\ \qquad + E[y_t a_t] - \phi E[t_t a_{t-1}] \\ r_{y1} = \phi_1 r_0 + \phi_2 r_1 - \kappa\theta E[y_{t-1}\varepsilon_{t-1}] \\ \qquad - \phi E[y_{t-1} a_{t-1}] \\ r_{y2} = \phi_1 r_1 + \phi_2 r_0 \end{cases} \tag{A2}$$

and

$$\begin{cases} E[y_t\varepsilon_t] = \kappa\sigma_\varepsilon^2 \\ E[y_t\varepsilon_{t-1}] = \phi_1 E[\varepsilon_t y_t] - \kappa\theta\sigma_\varepsilon^2 \\ E[y_t a_t] = \sigma_a^2 \\ e[y_t a_{t-1}] = \phi_1 E[a_t y_t] - \phi\sigma_a^2, \end{cases}$$

where $r_{yk} = E[y_t y_{t-k}]$ is the $k$-lag autocovariance of process $y_t$. Let $A = \kappa\sigma_\varepsilon^2$, $B = (\phi_1 - \theta)A$, $C = \sigma_a^2$, $D = (\phi_1 - \phi)C$, $E = \kappa A - \kappa\theta B + C - \phi D$, $F = -\kappa\theta A - \phi C$. Solve Equation (A2) for $r_{y0}$, $r_{y1}$, and $r_{y2}$, which yields

$$\begin{cases} r_{y0} = \dfrac{((-F - \phi_2 F)\phi_1 - E + \phi_2 E)}{((1+\phi_2)\phi_1^2 + \phi_2^2 - \phi_2^3 - 1 + \phi_2)} \\ r_{y1} = -\dfrac{(-\phi_2^2 F + F + \phi_1 E)}{(1+\phi_2)(\phi_1 - 1 + \phi_2)(\phi_1 + 1 - \phi_2)} \\ r_{y2} = -\dfrac{(\phi_1^2 E + (\phi_2 F + F)\phi_1 + \phi_2 E - \phi_2^2 E)}{((1+\phi_2)\phi_1^2 + \phi_2^2 - \phi_2^3 - 1 + \phi_2)}. \end{cases}$$

The autocovariance for $k \geq 3$ can be generated according to the following recursive equation:

$$r_{yK} = \phi_1 r_{y,k-1} + \phi_2 r_{y,k-2}.$$

It should be noted that the above calculation is valid for a stationary process only. The stability region of the output process is

$$\phi_1 + \phi_2 < 1, \quad \phi_2 - \phi_1 < 1, \quad |\phi_2| < 1.$$

## Appendix B
## The Autocovariance Structure of the Input Process

The input process follows an ARMA(1, 1) time-series model, as shown below:

$$x_t = \phi x_{t-1} + \varepsilon_t - \theta\varepsilon_{t-1}.$$

Let $r_{xk} = E[x_t x_{t-k}]$ be the $k$-lag autocovariance of process $x_t$. It is known that

$$\begin{cases} r_{x0} = \sigma_\varepsilon^2 \dfrac{1 - 2\phi\theta + \theta^2}{1 - \phi^2} \\ r_{xk} = \sigma_\varepsilon^2 \dfrac{(\phi - \theta)(1 - \phi\theta)}{1 - \phi^2}\phi^{k-1}, \quad k \geq 1. \end{cases}$$

It should be noted that the above calculation is valid for a stationary process only. The stationary condition for the input process is

$$|\phi| < 1.$$

## Appendix C
## The Covariance Structure Between the Input and Output Processes

Equation (3) is copied here for convenience:

$$y_t = \delta y_{t-1} + g(1-\delta)x_t + a_t. \tag{C1}$$

Multiplying both sizes of Equation (C1) by $y_{t-k}$, $k \geq 0$, and determining the expectation yields

$$r_{t(t-k)} = \begin{cases} (r_{yk} - \delta r_{y(k-1)} - \sigma_a^2)/\kappa & \text{for } k = 0 \\ (r_{yk} - \delta r_{y(k-1)})/\kappa, & \text{for } k \geq 1 \end{cases}$$

where $r_{ij} = \text{cov}(x_i, y_j)$. Multiplying both sides of (C1) by $x_{t-k}$, $k \geq 1$, and taking the expectation yields

$$r_{(t-k)t} = \delta r_{(t-k-1)t} + \kappa r_{xk}, \quad \text{for } k \geq 1.$$

The above equation can be computed recursively.

## References

ALWAN, L. C. and ROBERTS, H. V. (1989). "Time Series Modeling for Statistical Process Control". *Journal of Business & Economic Statistics* 6, pp. 87–95.

APLEY, D. W. and SHI, J. (1999). "The GLRT for Statistical Process Control of Autocorrelated Processes". *IIE Transactions* 31, pp. 1123–1134.

APLEY, D. W. and TSUNG, F. (2002). "The Autoregressive T-2

Chart for Monitoring Univariate Autocorrelated Processes". *Journal of Quality Technology* 34, pp. 80–96.

BASSEVILLE, M. and NIKIFOROV, I. V. (1993). *Detection of abrupt changes: theory and application*. Prentice Hall, Englewood Cliffs, N.J.

BOX, G. E. P. and LUCENO, A. (1997). *Statistical Control by Monitoring and Feedback Adjustment*. Wiley, New York, NY.

HAMILTON, J. D. (1994). *Time Series Analysis*. Princeton University Press, Princeton, NJ.

HAWKINS, D. M. (1993). "Regression Adjustment for Variables in Multivariate Quality Control". *Journal of Quality Technology* 25, pp. 170–182.

JIANG, W. (2004a). "A Joint Monitoring Scheme for Automatically Controlled Processes". *IIE Transactions* 36, pp. 1201–1210.

JIANG, W. (2004b). "Multivariate Control Charts for Monitoring Autocorrelated Processes". *Journal of Quality Technology* 36, pp. 367–379.

JONES, L. A.; CHAMP, C. W.; and RIGDON, S. E. (2004). "The Run Length Distribution of the CUSUM with Estimated Parameters". *Journal of Quality Technology* 36, pp. 95–108.

LIN, W. S. W. and ADAMS, B. M. (1996). "Combined Control Charts for Forecast-Based Monitoring Schemes". *Journal of Quality Technology* 28, pp. 289–301.

LOWRY, C. A. and MONTGOMERY, D. C. (1995). "A Review of Multivariate Control Charts". *IIE Transactions* 27, pp. 800–810.

LOWRY, C. A.; WOODALL, W. H.; CHAMP, C. W.; and RIGDON, S. E. (1992). "A Multivariate Exponentially Weighted Moving Average Control Cchart". Technometrics 34, pp. 46–53.

LU, C. W. and REYNOLDS, M. R. (1999). "EWMA Control Charts for Monitoring the Mean of Autocorrelated Processes". *Journal of Quality Technology* 31, pp. 166–188.

MASON, R. L.; TRACY, N. D.; and YOUNG, J. C. (1995). "Decomposition of T-2 for Multivariate Control Chart Interpretation". *Journal of Quality Technology* 27, pp. 99–108.

MASON, R. L. and YOUNG, J. C. (1999). "Improving the Sensitivity of the T-2 Statistic in Multivariate Process Control". *Journal of Quality Technology* 31, pp. 155–165.

MONTGOMERY, D. C.; KEATS, J. B.; YATSKIEVITCH, M.; and MESSINA, W. S. (2000). "Integrating Statistical Process Monitoring with Feedforward Control". *Quality and Reliability Engineering International* 16, pp. 515–525.

MONTGOMERY, D. C. and MASTRANGELO, C. M. (1991). "Some Statistical Process Control Methods for Autocorrelated Data". *Journal of Quality Technology* 23, pp. 179–193.

NEMBHARD, H. B. and KAO, M. S. (2003). "Adaptive Forecast-Based Monitoring for Dynamic Systems". *Technometrics* 45, pp. 208–219.

RUNGER, G. C. (2002). "Assignable Causes and Auto Correlation: Control Charts for Observations or Residuals?" *Journal of Quality Technology* 34, pp. 165–170.

SHU, L. J.; TSUNG, F.; and TSUI, K. L. (2004). "Run-Length Performance of Regression Control Charts with Estimated Parameters". *Journal of Quality Technology* 36, pp. 280–292.

TSUNG, F. and APLEY, D. W. (2002). "The Dynamic T-2 Chart for Monitoring Feedback-Controlled Processes". *IIE Transactions* 34, pp. 1043–1053.

TSUNG, F.; WU, H. Q.; and NAIR, V. N. (1998). "On the Efficiency and Robustness of Discrete Proportional-Integral Control Schemes". *Technometrics* 40, pp. 214–222.

TUCKER, W. T.; FALTIN, F. W.; and VANDERWIEL, S. A. (1993). "Algorithmic Statistical Process-Control—An Elaboration". *Technometrics* 35, pp. 363–375.

WANG, K. and TSUNG, F. (2007). "Monitoring Feedback-Controlled Processes Using Adaptive T2 Schemes". *International Journal of Production Research*, in press.

WOODALL, W. H. and NCUBE, M. M. (1985). "Multivariate CUSUM Quality-Control Procedures". *Technometrics* 27, pp. 285–292.

YASHCHIN, E. (1995). "Likelihood Ratio Methods for Monitoring Parameters of a Nested Random Effect Model". *Journal of the American Statistical Association* 90, pp. 729–738.

ZHANG, N. F. and POLLARD, J. F. (1994). "Analysis of Autocorrelations in Dynamic Processes". *Technometrics* 36, pp. 354–368.

ZHOU, S.; JIN, N.; and JIN, J. (2005). "Cycle-Based Signal Monitoring Using a Directionally Variant Multivariate Control Chart System". *IIE Transactions* 37, pp. 971–982.

$\sim$